Available online at www.sciencedirect.com
SCIENCE DIRECT®
Advances in Space Research 36 (2005) 1835–1839
ADVANCES IN SPACE RESEARCH
(a COSPAR publication)
www.elsevier.com/locate/asr

Energetic particle acceleration during a major magnetic storm

R. Kerttula [a], K. Mursula [a], T. Asikainen [a,*], R. Friedel [b], D. Baker [c], F. Søraas [d], J.F. Fennell [e], J.B. Blake [e], M. Grande [f]

[a] Department of Physical Sciences, P.O. Box 3000, FIN-90014, University of Oulu, Finland
[b] LANL, NIS-2, MS 426, Los Alamos, NM 87544, USA
[c] Laboratory for Atmospheric & Space Physics, University of Colorado, Boulder 1234 Innovation Drive Boulder CO 80303, USA
[d] University of Bergen, Department of Physics, Allegates 55, N-5007 Bergen, Norway
[e] Mail Stop M2-259, The Aerospace Corp., P.O. Box 92957, Los Angeles, CA 90009, USA
[f] Space Physics Division, Space Science and Technology Department, CCLRC Rutherford Appleton Laboratory, Chilton, Didcot, Oxfordshire, OX11 0QX, UK

Received 21 December 2002; received in revised form 25 March 2004; accepted 26 March 2004

Abstract

We study the global properties of energetic (>30 keV) particles during the main and early recovery phase of a major magnetic storm of March 31, 2001, using data of the NOAA 15 and 16 and the CLUSTER satellites. During the storm main phase the ring current energetic electron and ion fluxes were increased by nearly two orders of magnitude, and the flux maxima were shifted to below $L = 3$. The maximum ion fluxes were observed at about 07 UT, coinciding with the minimum Dst. However, the highest fluxes of energetic electrons were observed only at about 16–18 UT, indicating significant differences in the acceleration of energetic electrons and ions during the storm. We suggest that the ion maximum at about 07 UT was due to field-aligned acceleration of ions from the ionosphere whereas the electron maximum at 16–18 UT was due to a large injection from the nightside.

Keywords: Magnetic storm; Energetic particle injections; Energetic particle boundaries

1. Introduction

Geomagnetic storms are known to enhance the ring current (RC) strength, which is mostly due to new ions appearing at $L < 4$ (Smith and Hoffman, 1973; Hamilton et al., 1988; Korth and Friedel, 1997). Particularly during major magnetic storms the RC intensification is mostly provided by O^+ ions of ionospheric origin (Hamilton et al., 1988; Daglis, 1997), and oxygen ions can be the main ion species during the main phase of intense storms. In this paper we will analyse both electron and ion dynamics during a great storm of March 31, 2001, and show that they depicted a surprisingly different behaviour during this storm.

* Corresponding author.
E-mail address: timo.asikainen@oulu.fi (T. Asikainen).

0273-1177/$30 © 2005 Published by Elsevier Ltd on behalf of COSPAR.
doi:10.1016/j.asr.2004.03.023

2. Instrumentation

In this study, we use energetic particle data from the Medium Energy Proton and Electron Detector (MEPED) instrument onboard the NOAA 15 and 16 satellites. Ions (no mass separation is provided) and electrons are measured separately at roughly vertical (0°) and horizontal (90°) directions with 30° field of view. Note that at high (low) latitudes the 0° detector measures mostly precipitating (trapped) particles and vice versa for the 90° detector. The MEPED instrument has six energy channels for ions (from 30–80 to >7000 keV) and three for electrons (from >30 to >300 keV). The NOAA 15 and 16 orbits are circular at an altitude of about 850 km. The orbital plane is 20–08 MLT for NOAA 15 and 14–02 MLT for NOAA 16 (see Evans and Greer, 2000, for more details of the MEPED instrument).

The Research with Adaptive Particle Imaging Detectors (RAPID) spectrometer for the Cluster mission analyzes suprathermal plasma distributions in the energy range from 20 to 400 keV for electrons, 40–1500 keV for protons and 10–1500 keV/nuc for heavier ion species The RAPID instrument uses two different and independent detector systems for the detection of nuclei and electrons: Imaging Ion Mass Spectrometer (IIMS) and Imaging Electron Spectrometer (IES) (see Wilken et al., 1997, for a more detailed description of the RAPID instrument).

3. Observations

3.1. Storm overview

On March 31, 2001, the Advanced Composition Explorer (ACE) satellite was measuring interplanetary conditions at about (223, −23. −12) R_E. As shown in Fig. 1, IMF Bz component was fluctuating between large positive and negative values until about 04 UT when the direction changed southwards for about three hours. Strongest negative values (<−40 nT) were observed around 06 UT. The solar wind (SW) velocity increased between 00 and 02 UT in two steps from about 400 to above 750 km/s. Solar wind dynamic pressure, which mainly followed the changes in SW density, showed dramatic variations during the first six hours of the day. At about 0020 UT, it had a very sharp peak which lasted only about half an hour. Another, longer pressure increase occurred roughly from 02 to 06 UT. These interplanetary conditions led to the generation of a major (Dst = −360 nT) magnetic storm with a rapid main phase starting at 04 UT and ending at 08 UT. The extreme geomagnetic conditions can also be verified by the LANL geostationary satellite data (not shown here), which indicate that the magnetopause was pushed inside the geosynchronous orbit in the dayside roughly at about 03–08 UT and even in the morning and evening sectors at about 06 UT. After a period of positive values, the IMF Bz experienced another long interval of negative values at about 14–21 UT which caused a secondary minimum in Dst (−285 nT).

3.2. NOAA observations

The two NOAA satellites verify that both ion and electron fluxes were increased by nearly two orders of magnitude from the average level on March 30 to their storm time maxima. The maximum ion flux was at 05–07 UT while that of electrons occurred only at about 16–18 UT.

Fig. 2 plots the NOAA 16 90° ion fluxes versus L value for March 31, 2001. Each plot contains data from half a satellite orbit around the equator (negative L corresponding to the southern hemisphere). Data from each L shell width of 0.5 is averaged, leading to a changing time resolution along the orbit. The first and third (second and fourth) columns of plots present data from the postnoon (postmidnight) sector. Ion fluxes were systematically higher in the nightside than dayside until the end of the day. Fig. 2 shows that the flux maxima shifted

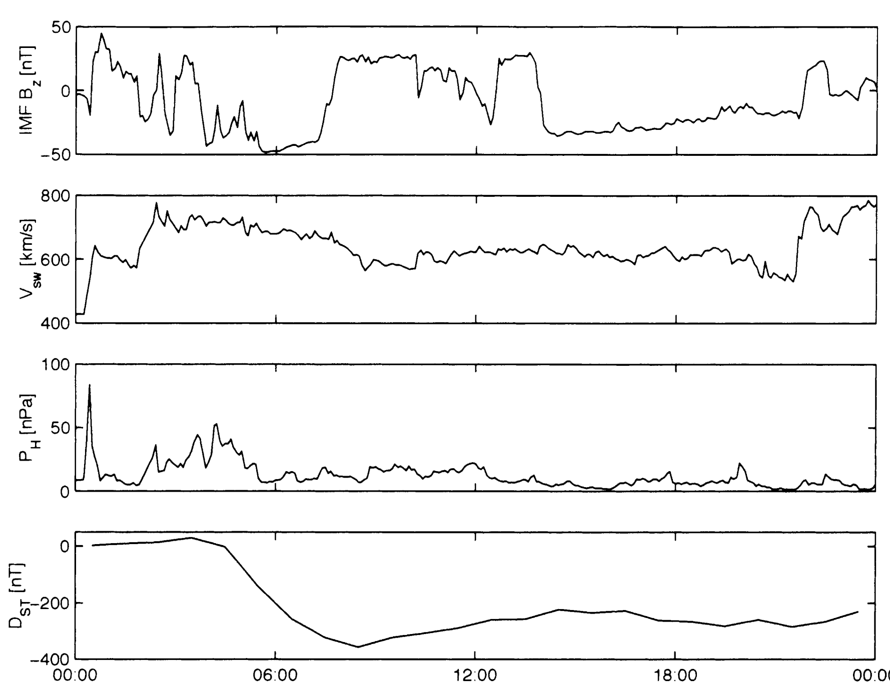

Fig. 1. ACE observations on March 31, 2001, of IMF Bz component, solar wind velocity, and solar wind pressure together with the Dst index.

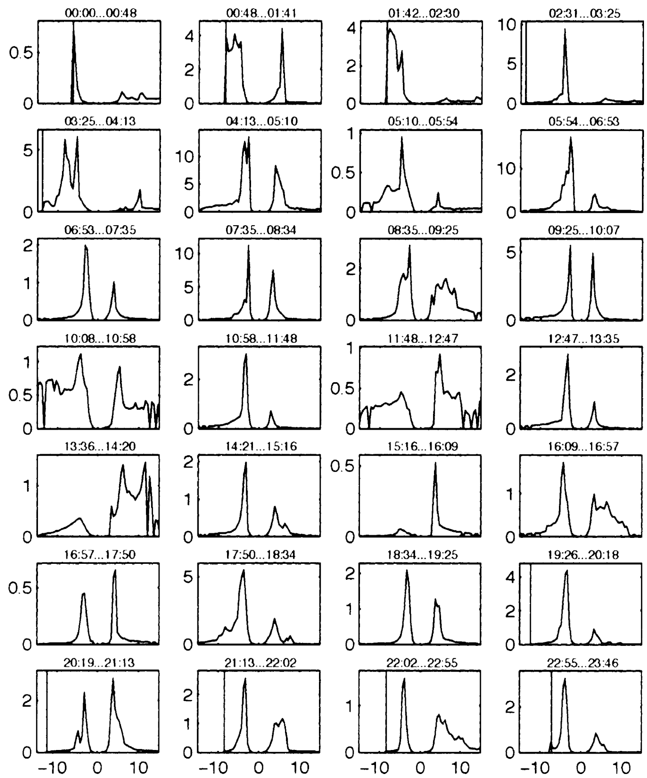

Fig. 2. NOAA 16 90° total ion fluxes (in units of 10^4 cm^{-2} s^{-1} sr^{-1}) presented in plots covering half an orbit around the equator. The first and third (second and fourth) columns of plots present data from the postnoon (postmidnight) sector. Respective times are given above each plot. Horizontal axis gives the L value with −10, 0 and 10 noted by tick marks. Occasional vertical lines denote the L shell extent of the orbit.

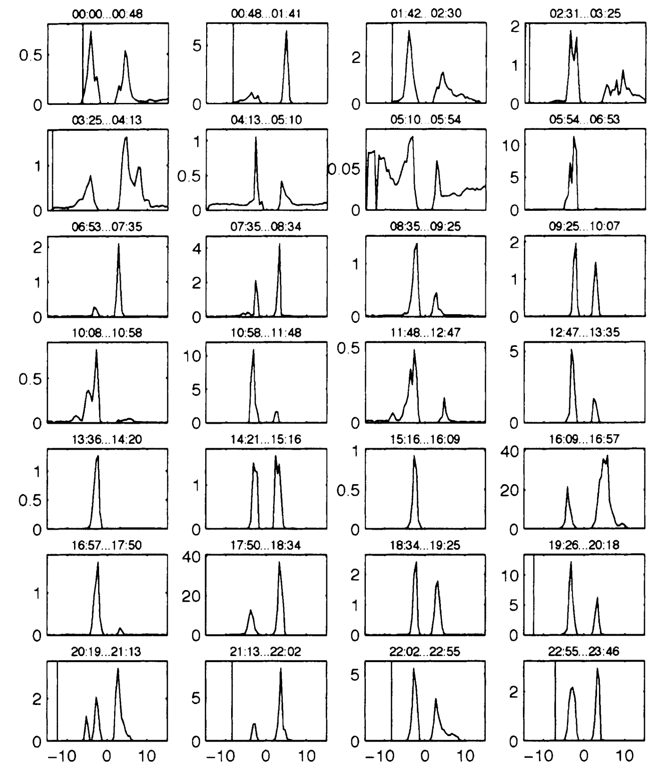

Fig. 3. NOAA 16 90° total electron fluxes presented as in Fig. 2.

inwards to below $L = 3$ from the start of the day until the end of the main phase. One can see that the nightside ion fluxes were fairly intense already at the start of the day, and were slightly enhanced at about 03–05 UT, staying at roughly the same level until about 08 UT and then decreasing slowly. No other major ion flux increases were observed at nightside. All these features are supported by the NOAA 16 0° channel (not shown).

At the dayside, NOAA 16 ion fluxes were enhanced at 02–04 UT. Note that this enhancement was very north-south asymmetric, with considerably larger fluxes in the southern hemisphere. Also, the flux maxima of this enhancement were found at a higher L shell than the maxima on orbits before or after the enhancement. AT NOAA 15 the ion flux maxima also shifted to low L shells during the main phase. At dusk the ion fluxes behaved slightly differently from NOAA 16 observations at nightside. The absolute flux maximum was attained at about 06 UT. Note that this maximum is larger at NOAA 15 (esp. in the 0° detector) than any other ion fluxes at the two NOAA satellites. Second, there was another ion flux maximum at dusk at about 16–18 UT. At dawn, there was a fairly strong ion enhancement at about 05–07 UT.

The evolution of NOAA 16 90° electron fluxes (see Fig. 3) shows some similar trends as ions, e.g., the fluxes tend to be higher at the nightside than at dayside and the flux maxima shifted toward inner L shells during the main phase. However, there are also some clear differences. Electron fluxes depicted considerably larger variability than ions. The initial flux level was greatly reduced until a new enhancement was observed about 0620 UT. Thereafter electron fluxes were decreased again until another enhancement occurred at about 1130 UT. No increase was seen at this time in ion fluxes. The absolute electron flux maximum at NOAA 16 was obtained at about 16–18 UT. As mentioned above, only a small increase was found in NOAA 16 ion fluxes at this time. However, the second ion flux maximum at dusk at NOAA 15 occurred at this time. Note also that there was no high-latitude dayside electron maximum in the southern hemisphere at 02–04 UT as found for ions. This would need a mechanism (e.g., a field-aligned potential) which can accelerate downward solar wind ions but not electrons.

Electron flux changes at NOAA 15 followed largely those at NOAA 16 but the variations were less dramatic. The enhancement at 07 UT was clearly seen in the morning sector but there was hardly any change at 11 UT. The largest enhancement occurred at about 17–19 UT mainly in the morning, in agreement with NOAA 16 observations at midnight.

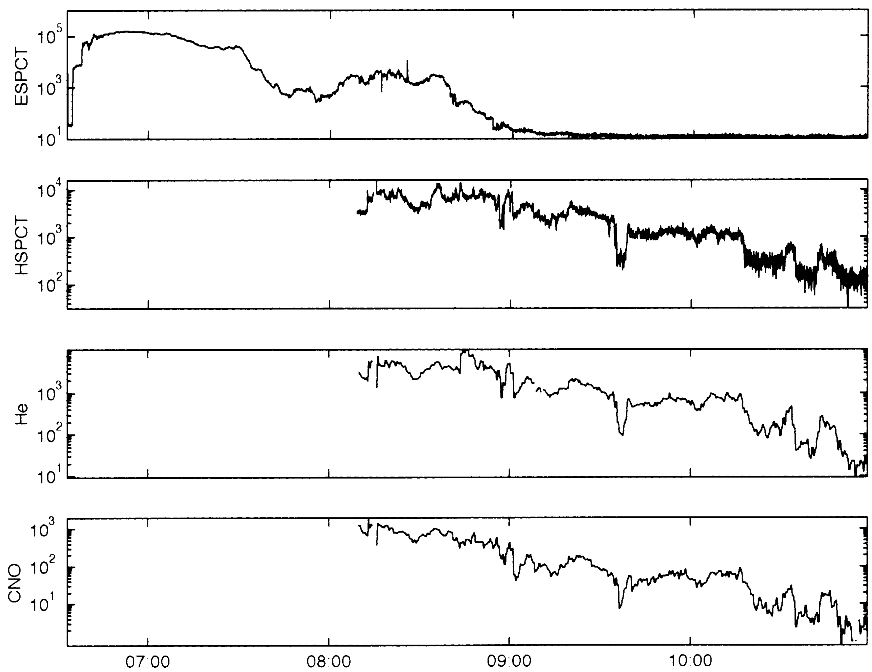

Fig. 4. Cluster s/cl RAPID total fluxes of energetic electrons, protons, helium and oxygen ions.

3.3. CLUSTER observations

The four Cluster satellites had their perigee at about 07 UT on March 31, 2001. The RAPID energetic particle spectrometer (Wilken et al., 1997, 2001) measured the electron fluxes around the perigee since about 0630 UT (see Fig. 4) and the three types of ions (protons, helium and oxygen ions) since about 0810 UT. Curiously, the Cluster perigee was in the 22 LT sector, i.e., inbetween the equatorial LT sectors of the two NOAA satellites.

Cluster observed a high flux of energetic electrons around the perigee from 0635 to 0845 UT (a detailed analysis of Cluster energetic electron observations at this time was made by Baker et al., 2002). The strongest fluxes were found around the Cluster perigee at about $L = 4$–5. This is in an excellent agreement with NOAA 16 (see Fig. 3) and NOAA 15 observations where the highest electron fluxes were restricted to below $L = 5$. After a weak minimum at about $L = 5$ Cluster observed a region of lower fluxes of energetic electrons until about $L = 12$. This structure could already be seen at NOAA 16 at about 05 UT (see the small plot in Fig. 3 corresponding to 0413…0510 UT) as well as at NOAA 15 later at about 08 UT, i.e., at the time of Cluster observations (note that the flux enhancement at NOAA 16 at about 0620 UT makes this structure less evident in Fig. 3 at this time).

4. Discussion and conclusions

We have seen that the RC particle populations were greatly intensified during the storm time from the average quiet time level. The ion flux maximum was found to well coincide with the Dst minimum time at the end of the main phase. This ion flux maximum was seen as a particularly strong enhancement by NOAA 15 in the dusk sector at about 0630 UT (the strong north–south asymmetric distribution implies a rapid temporal development). This enhancement cannot be explained by a drift of previously existing population from nightside monitored by NOAA 16. Instead, it is in a good agreement with the observation of intense flow of energetic, oxygen ions at 19 LT by the Fast satellite (Baker et al., 2002). Accordingly, the majority of NOAA ions at this time may well be heavy ions. Note also that there was a simultaneous strong ion enhancement in the morning sector observed by NOAA 15 which also cannot be understood in terms of drift.

It is well known that the oxygen ions may be the dominant ion species during the main phase of a storm (see e.g., Hamilton et al., 1988; Daglis, 1997). Fig. 4 also demonstrates the existence of a large flux of energetic oxygen ions far above the quiet time average (unfortunately, RAPID ion observations only started at about 0810 UT when satellites were already outside the main RC beyond $L = 6$). Therefore, the present observation by NOAA and Cluster satellites support the simultaneous Fast satellite observations. Also, the NOAA and Fast observations suggest for a large contribution to ring current during storm main phase directly from the ionosphere in the dusk sector (and probably also in the dawn sector), instead of a less direct route via storage and acceleration in the tail and subsequent drift.

In a dramatic difference to ions, the energetic electrons had their maximum fluxes only in the recovery phase of the storm in connection of a major substorm. Moreover, the largest electron fluxes were found by NOAA 16 in the night sector while the NOAA 15 fluxes at dawn could be well understood in terms of the standard view of eastward drift of electrons. These facts suggest that the flux maxima of energetic ions and electrons were formed by different mechanisms, the electron flux maxima by the standard tailside storage and acceleration, the ions mainly by the field-aligned acceleration of ionospheric ions.

The 06 UT field-aligned acceleration was hardly due to a static potential since it would require that the main acceleration occurred below the NOAA altitude. A potential above the satellites would also accelerate electrons for which there is no evidence at dusk. Therefore, we suggest that the field-aligned acceleration was more likely caused by the ion cyclotron waves which accelerate only ions. Moreover, this mechanism accelerates massive ions (oxygen ions) more effectively than protons, thus explaining the Fast observations. Note also that ion cyclotron waves have been observed to be greatly enhanced during the storm main phase (Bräysy et al., 1998).

Acknowledgements

The Academy of Finland is acknowledged for financial support. National Oceanic and Atmospheric Administration (NOAA), US Department of Commerce, is acknowledged for NOAA satellite data.

References

Baker, D.N., Ergun, R.E., Burch, J.L., et al. A telescopic and microscopic view of a magnetospheric substorm on 31 March 2001. Geophys. Res. Lett., 2002, doi:10.1029/2001GL014491.

Bräysy, T., Mursula, K., Marklund, G. Ion cyclotron waves during a great magnetic storm observed by Freja double-probe electric field instrument. J. Geophys. Res. 103, 4145–4155, 1998.

Daglis, I.A. The role of magnetosphere–ionosphere coupling in magnetic storm dynamics, in magnetic storms. in: Tsurutani, B.T. et al. (Eds.), Geophysical Monograph, 98. AGU, Washington, DC, pp. 107–116, 1997.

Evans, D.S., Greer, M.S. Polar orbiting environmental satellite space environment monitor – 2: instrument descriptions and archive data documentation. NOAA Technical Memorandum OAR SEC-93, Boulder, CO, 2000.

Hamilton, D.C., Gloeckler, G., Ipavich, F.M., Stüdemann, W., Wilken, B., Kremser, G. Ring current development during the great geomagnetic storm of February 1986. J. Geophys. Res. 93, 14343–14355, 1988.

Korth, A., Friedel, R.H.W. Dynamics of energetic ions and electrons between $L = 2.5$ and $L = 7$ during magnetic storms. J. Geophys. Res. 102, 14113–14122, 1997.

Smith, P.H., Hoffman, R.A. Ring current particle distributions during the magnetic storms of December 16–18, 1971. J. Geophys. Res. 78, 4731–4737, 1973.

Wilken, B., Axford, W.I., Daglis, I., et al. RAPID: the imaging energetic particle spectrometer on Cluster. Space Sci. Rev. 79, 399–473, 1997.

Wilken, B., Daly, P.W., Mall, U., et al. First results from the RAPID imaging energetic particle spectrometer on board Cluster. Ann. Geophys. 19, 1355–1366, 2001.